

Compression Zone Effect in Batch Sedimentation

Theories of batch sedimentation, taking into account the compression zone effect, are reinterpreted and modified. According to the discussion presented and the experimental results shown, characteristics—which are the loci of points representative of layers with the same settling rate and the same solids concentration in the settling zone—rise tangentially to the sediment curve on a height vs. time plot. Mathematical expressions that relate the solids concentration to the variations of the pulp-supernatant interface height and of the sediment height are presented. In addition, the model presented is proposed for use when it is not possible to measure the sediment height. A procedure for calculating the concentration at the top of the sediment is also indicated.

Calcium carbonate suspensions in water were selected for testing the equations deduced. The relation between the continuous thickener unit area and the underflow solids concentration was obtained from the batch tests, and is compared with that calculated by the graphic methods of Talmadge and Fitch, and Fitch.

R. Font

División de Ingeniería Química
Facultad de Ciencias
Universidad de Alicante
Apartado 99, Alicante, Spain

Introduction

For many years, the design of gravity thickeners has been based upon the work of Coe and Clavenger (1916) and Kynch (1952), as modified by Talmadge and Fitch (1955). The Kynch procedure is attractive because from only one test it is possible to obtain a relationship between the settling rate and the concentration of solids.

Recently, the effect of the rising compression zone upon the Kynch method has been considered. Tiller (1981) has developed a useful mathematical method to correlate the solids concentration of the layers that reach the supernatant-suspension interface as a function of the variations of the supernatant-pulp interface height and the compression discontinuity height vs. time. However, with Tiller's procedure it is not possible to obtain a relation between the settling rate and the solids concentration from one laboratory test. Tiller's paper does not recognize that the characteristics (lines whose points correspond to layers with the same solids concentration and the same settling rate) rise tangentially to the sediment surface curve in a height vs. time plot.

Fitch (1983) deduced that every characteristic that rises from the sediment does so tangentially, but he does not explain the

satisfactory results obtained by Tiller without this assumption. Nevertheless, Fitch does not use the equations deduced by Tiller and proposes others, which are discussed in this paper. In any case, the Tiller and Fitch procedures involve measuring the variation of the compression zone height vs. time and therefore their applicability is limited.

The objectives of this work have been the following:

- To analyze the assumptions presented by Tiller (1981) and Fitch (1983)
- To develop and discuss a mathematical model that may be used to work out the relation between the settling rate and the solids concentration
- To calculate the solids concentration at the top of the sediment
- To determine from the data of a batch test the relation between the unit area of continuous thickener and the underflow solids concentration

The rise of the compression interface is usually not visible. Fitch (1983) has proposed a method based on the determination of the critical points of several tests with different initial heights. One of the aims of this paper has been to develop a method to estimate the variation of the sediment height with time when the compression zone is not visible.

Revision of Theory

Batch laboratory sedimentation tests are frequently performed in graduated cylinders. Most of the data reported in the literature refer only to the descending upper phase boundary and omit the equally important rising compression zone. Recently, some researchers have analyzed the influence of the sediment in the method to calculate the relationship between the settling rate and the solids concentration.

The development of this paper is based on Kynch's theorems, which are analyzed by Fitch (1983). It is also assumed that the great change of solids concentration corresponding to a mathematical discontinuity takes place in a very thin zone. It is also recognized that the settling rate of a layer only depends on the solids concentration in the settling zone, Figure 1. In the sediment or compression zone the subsidence velocity of solids depends on the solids concentration as well as the squeeze transmitted by the upper layers.

Tiller (1981) presented a mathematical model that relates some variables. In Figure 1 the sediment height L_1 and the pulp-supernatant interface height H_2 are plotted vs. times t_1 and t_2 , respectively. According to Tiller's model, the straight characteristic line drawn from (t_1, L_1) to (t_2, H_2) represents the rise of a layer with constant volume fraction ϕ_{s2} .

Using the jump boundary condition in the sediment interface (d'Avila and Sampaio, 1979), Tiller obtained the following equation:

$$\int_0^{L_1} \frac{\partial \epsilon_s}{\partial t_1} dx + \epsilon_{s1} \frac{dL_1}{dt_1} = \phi_{s2} \left(-\frac{dH_2}{dt_2} + \frac{dL_1}{dt_1} \right) \quad (1)$$

Another relation between the variables indicated in Figure 1 is the following:

$$\phi_{s2} = \frac{\phi_{s0} H_0}{H_{12} - L_1} \exp \left[\int_0^{t_1} \frac{\frac{dH_2}{dt_2} - \frac{dL_1}{dt_1}}{H_{12} - L_1} dt_1 \right] \quad (2)$$

Equation 2 was deduced by Tiller and corrected by Fitch

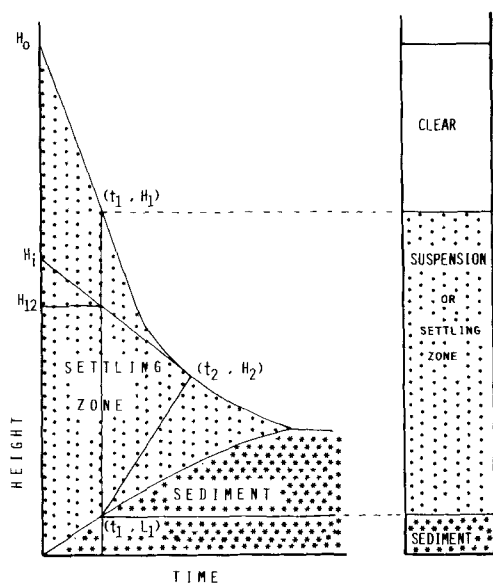


Figure 1. Interface in batch sedimentation.

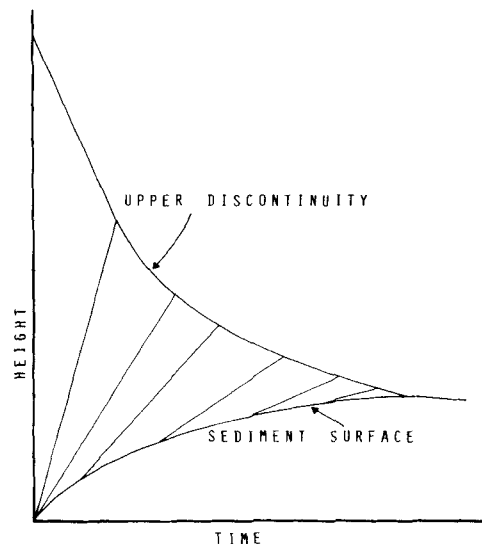


Figure 2. Possible rise of characteristics.

(1982). Tiller applied Eq. 2 to attapugite sedimentation data by trial-and-error selection of a set of characteristic lines. Values worked out from the slope ν_1 of his characteristics, using Eq. 2, agree quite well with his experimental values.

The relation pointed out by Eq. 2 is valid for any set of characteristics drawn with decreasing slope, as in the case illustrated in Figure 2. In Appendix I of the supplementary material a demonstration is presented in which the following expression is deduced from the above equations:

$$\nu_1 = \frac{H_2 - L_1}{t_2 - t_1} = \frac{d(\phi_{s2} u_{s2})}{d\phi_{s2}} = \frac{d[\phi_{s2}(dH_2/dt_2)]}{d\phi_{s2}} \quad (3)$$

That means that any set of characteristics drawn as shown in Figure 2 is in accordance with Kynch's theorems. Therefore, from one batch test we can obtain infinite relations between the settling rate and the solids concentration. All these relations are possible and consequently one batch test is not sufficient to determine uniquely $u_s = f(\phi_s)$, if no information is available on the rise of the characteristics.

Solids at the top of the compressible sediment will always have the volume fraction ϵ_{s1} at which the solids structure first shows compressive yield value. If the solids are compressive, the sedimentation rate just below the compression discontinuity will not be zero except initially, when the depth of the compression zone is small.

According to Kynch's theory, the rise velocity of a discontinuity v is:

$$v = \frac{\Delta S}{\Delta c_s} \quad (4)$$

The velocity of the rising sediment dL_1/dt_1 can be deduced from Eq. 1 or from Eq. 4 applied to the sediment surface, as follows:

$$\frac{dL_1}{dt_1} = \frac{\phi_{s2} \left(\frac{dH_2}{dt_2} \right) - \left(-\int_0^{L_1} \frac{\partial \epsilon_s}{\partial t_1} dx \right)}{\phi_{s2} - \epsilon_{s1}} = \frac{\phi_{s2} u_{s2} - \epsilon_{s1} u_{s1}}{\phi_{s2} - \epsilon_{s1}} \quad (5)$$

In Eq. 5 $-\int_0^{L_1} (\partial \epsilon_s / \partial t_1) dx$ is the volumetric flux of solids, corresponding to the sediment, and it equals the product of ϵ_{s1} times u_{s1} (sedimentation velocity of the solids at cake surface).

Fitch (1983) presented a valid discussion of the stability of the discontinuities. He affirmed that every characteristic line that rises from the sediment is tangent to the curve $L_1 = f(t_1)$. The experimental results of this paper confirm this hypothesis.

Another valid reason explaining the rise of the characteristics is the following. Consider the three cases illustrated in Figure 3. u_{s1} is the sedimentation velocity of the upper layer of the sediment, and ϵ_{s1} is the volume fraction of the same layer. Points A, B, and C correspond to the parameters representative of the layer in the settling zone just above the sediment surface for the three cases, respectively. According to Eq. 5, dL_1/dt_1 equals the slope of the segment that joins the points representative of the layers just above and below the sediment surface. The velocity of the characteristic that rises from the sediment is the slope of the tangent at each point. In case A the slope of the characteristic equals dL_1/dt_1 . In case B the rise velocity of the characteristic is less than the velocity of the rising sediment, and consequently this situation cannot occur. In case C the rise velocity of the characteristic is greater than the velocity of the rising sediment. This case can correspond to the situation shown in Figure 2. In this latter case, there is a greater change of sedimentation velocity of the particles crossing the compression zone discontinuity than that of point A. There is no reason that justifies this great change. Nevertheless the inertial effects of the particles, although they are very small, can impede a great change of velocity, and consequently characteristics must rise tangentially to the sediment.

Corrected Model

In a batch sedimentation test as drawn in Figure 4, three zones can be considered. In zone (a) the volume fraction ϕ_i is the initial one, ϕ_{s0} . In zone (b) all the characteristics rise from the bottom of the cylinder. According to Kynch's theory, ϕ_s can be

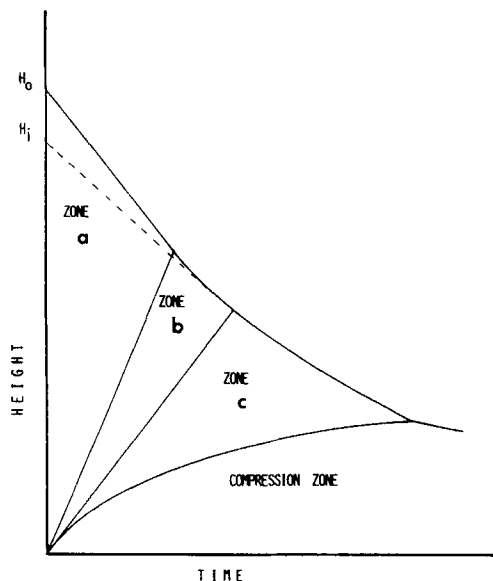


Figure 4. Zones in a height vs. time plot.

worked out by the following equation:

$$\phi_s = \frac{\phi_{s0} H_0}{H_i} \quad (6)$$

In zone (c) all the characteristics rise tangentially from the sediment. In this case Eq. 2 must be used to calculate the corresponding value ϕ_{s2} of the characteristic that reaches the pulp-supernatant discontinuity. In Figure 5 the variables used in this paper are illustrated. Note that the variables related to the characteristic that rises from the bottom tangentially to the sediment have an asterisk. Taking into account that the characteristics rise tangentially from the sediment, Eq. 2 can be simplified as follows.

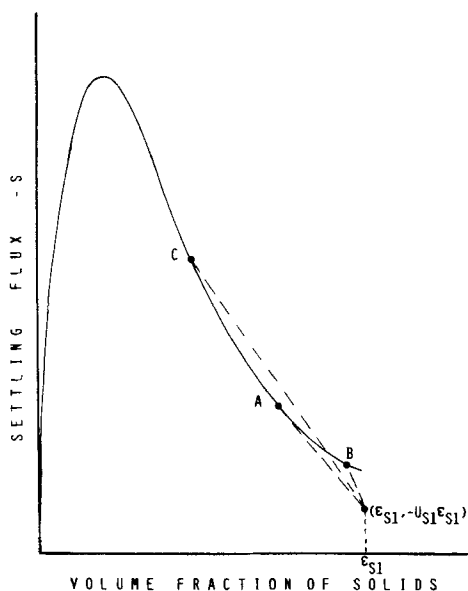


Figure 3. Rise of characteristics.

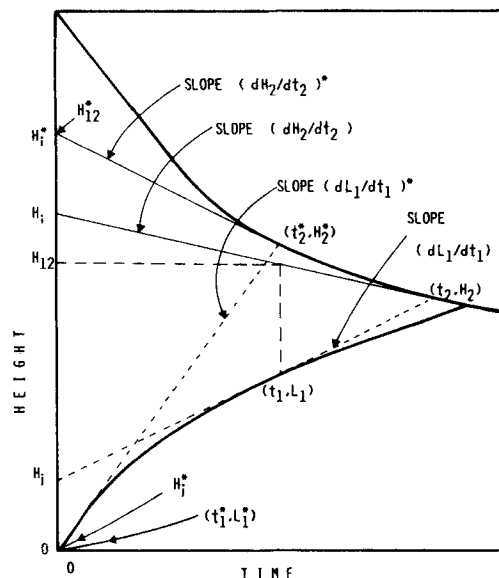


Figure 5. Interfaces and characteristics in batch sedimentation: nomenclature.

From Figure 5

$$\frac{dH_2}{dt_2} = \frac{H_2 - H_{12}}{t_2 - t_1} \quad (7)$$

From Eqs. 3 and 7 and considering that $v_1 = (dL_1/dt_1)$,

$$\frac{\frac{dH_2}{dt_2} - \frac{dL_1}{dt_1}}{H_{12} - L_1} = \frac{\frac{H_2 - H_{12}}{t_2 - t_1} - \frac{H_2 - L_1}{t_2 - t_1}}{H_{12} - L_1} = -\frac{1}{t_2 - t_1} \quad (8)$$

From Eqs. 2 and 8

$$\phi_{s2} = \frac{\phi_{s0} H_o}{H_{12} - L_1} \exp\left(-\int_0^{t_1} \frac{1}{t_2 - t_1} dt_1\right) \quad (9)$$

This equation is different from the one obtained by Fitch (1983), given below as Eq. 30, where by geometrical construction a hypothetical characteristic line is drawn from the x axis to the curve $L_1 = f(t_1)$.

Concentration at the top of the compression zone

From the equations presented previously the volume fraction ϵ_{s1} of the upper limit of the sediment can be worked out. At time $t_1 = 0$ the sedimentation velocity u_{s1} of the sediment is zero because there are no solids in the incipient sediment that compress themselves. Applying Eq. 5 when $t_1 = 0$ and taking into account that $u_{s1} = 0$, the following equation can be deduced:

$$\epsilon_{s1} = \frac{\phi_{s2}^* \left[\left(-\frac{dH_2}{dt_2} \right)^* + \left(\frac{dL_1}{dt_1} \right)^* \right]}{\left(\frac{dL_1}{dt_1} \right)^*} \quad (10)$$

From Figure 5

$$-\left(\frac{dH_2}{dt_2} \right)^* = \frac{H_i^* - H_2^*}{t_2^*} \quad (11)$$

and

$$\left(\frac{dL_1}{dt_1} \right)^* = \frac{H_2^*}{t_2^*} \quad (12)$$

Substituting Eqs. 11 and 12 in Eq. 10, we obtain

$$\epsilon_{s1} = \frac{\phi_{s2}^* H_i^*}{H_2^*} \quad (13)$$

The product $\phi_{s2}^* H_i^*$ equals $\phi_{s0} H_o$ because the first characteristic that rises from the sediment also does so from the bottom, and therefore Eq. 13 becomes

$$\epsilon_{s1} = \frac{\phi_{s0} H_o}{H_2^*} \quad (14)$$

Continuous thickening

The continuous-thickening design has been considered by many authors (Coe and Clavenger, 1916; Talmadge and Fitch,

1955; Scott, 1966, 1968; Fitch, 1966, 1975, 1979, 1983). The information that can be obtained by applying the equations presented previously, will be discussed here in order to determine the continuous-thickener area.

From a batch test, values of u_s as a function of ϕ_s in an interval of concentrations can be obtained. The volumetric settling flux of solids S that can be worked out is drawn in Figure 6. Dashed lines represent the part that cannot be obtained from a single test. The part of the curve $S = f(\phi_s)$ that can be determined depends on the initial volume fraction ϕ_{s0} . In Figure 6 a common case is considered.

Continuous thickening can be represented in a flux plot by a Yoshioka construction (Yoshioka et al., 1957), Figure 6. A material balance line is drawn from ϵ_{su} (at the bottom) tangentially to the curve $-S = f(c_s)$. The intercept of this line on the $-S$ axis is the maximum possible thickener flux $-\theta$.

Fitch (1983) has presented an analysis of the compression discontinuity in a continuous thickener. According to this analysis, the upward propagation velocity v_c of the compression discontinuity with respect to the suspension must be equal to the downward velocity v_u imparted to the system by underflow withdrawal. The value v_u equals $-\theta/\epsilon_{su}$ (volumetric flux divided by volume fraction of solids in the underflow stream). The propagation velocity v_c of the cake surface equals $\Delta S/\Delta c_s$, according to one of Kynch's theorems, and consequently

$$v_c = v_u = \frac{-\theta}{\epsilon_{su}} = \frac{\Delta S}{\Delta c_s} = \frac{u_{s2}\phi_{s2} - u_{s1}\epsilon_{s1}}{\phi_{s2} - \epsilon_{s1}} \quad (15)$$

where ϕ_{s2} and ϵ_{s1} are the volume fraction of solids above and below the compression discontinuity in the continuous thickener.

From Figure 6 and according to the Yoshioka construction, we deduce

$$v_u = \frac{u_{s2}\phi_{s2} - u_{s1}\epsilon_{s1}}{\phi_{s2} - \epsilon_{s1}} = \frac{u_{s2}\phi_{s2}}{\phi_{s2} - \epsilon_{su}} \quad (16)$$

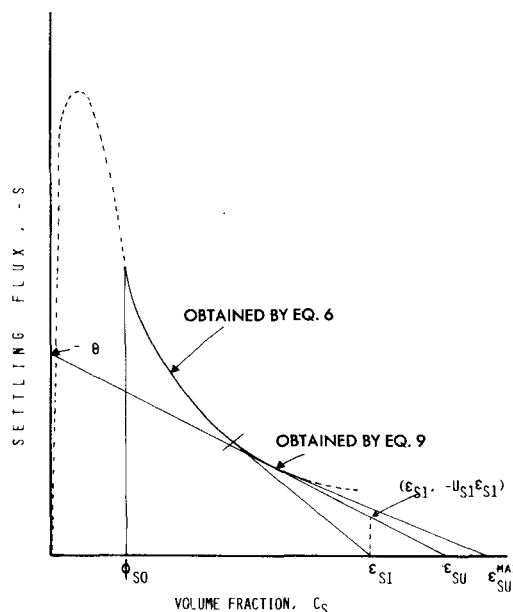


Figure 6. Yoshioka construction for continuous thickening.

If the usual Talmadge and Fitch procedure is followed, or from Eq. 16, we obtain

$$\epsilon_{su} = \phi_{s2} \left(1 + \frac{-u_{s2}}{v_u} \right) \quad (17)$$

Comparing Eq. 15 or Eq. 16—equations applied to continuous thickeners—with Eq. 5, applied to batch tests, we deduce that the relation between ϕ_{s2} and ϵ_{su} in a continuous thickener can be obtained from a batch test if $v_u = dL_1/dt_1$. Therefore Eq. 17 can be written as

$$\epsilon_{su} = \phi_{s2} \left[1 + \frac{-u_{s2}}{(dL_1/dt_1)} \right] \quad (18)$$

The value v_u equals $-\theta/\epsilon_{su}$, and consequently from Eq. 15

$$-\theta = \left(\frac{dL_1}{dt_1} \right) \epsilon_{su} \quad (19)$$

From Figure 6 one deduces that the maximum value ϵ_{su}^{max} at the bottom of the thickener (that can be designed using the experimental data obtained from a batch test), corresponds to the minimum value of dL_1/dt_1 (at the critical point). If the required concentration of the thickener underflow is less than the value ϵ_{su}^{max} , the procedure to work out the relation between the unit area of the continuous thickener and the solids volume fraction of the thickener underflow is the following. ϕ_{s2} and $-u_{s2}$ ($= -dH_2/dt_2$), corresponding to the characteristic with slope dL_1/dt_1 , are calculated using Eq. 9 for different values of dL_1/dt_1 . Next, using Eq. 18 ϵ_{su} is worked out, and afterward $-\theta$ from ϵ_{su} using Eq. 19. The unit area A_u equals $1/-\theta$.

Physical significance of ϵ_{su}

In the cake formed on the bottom of the column in a batch test, there is a gradient of volume fraction of solids between ϵ_{s1} and another greater value. At the beginning of the test, the solids volume fraction of the initial sediment is ϵ_{s1} . Later the weight of the solids compresses the lower layers, and consequently lines of equal concentration ϵ_s greater than ϵ_{s1} rise from the bottom. At time infinite, all the solids are in the compression zone, the sedimentation rates of all the layers equal zero, and the concentration of each layer depends on the compression stress transmitted by the upper layers.

In the following analysis, a hypothetical situation is considered. It is assumed that as long as the sediment is building up on the bottom, the solids concentrations of the sediment layers are the maximum possible in accordance with the squeeze transmitted by the upper layers. In this hypothetical situation ϵ_s depends only on the mass of solids above the layer considered. This is equivalent to admitting that the sedimentation rate is infinite when the squeeze transmitted is greater than the maximum that could be supported without subsidence of the layer, and that the sedimentation rate is zero when the squeeze transmitted equals the maximum allowed without subsidence of the layer. Therefore, in this extreme case lines of equal concentration are equidistant to the curve $L_1 = f(t_1)$, as shown in Figure 7, and consequently ϵ_s is only a function of the distance z to the sediment surface.

If V_s is the volume of all the solids by unit of cross section in

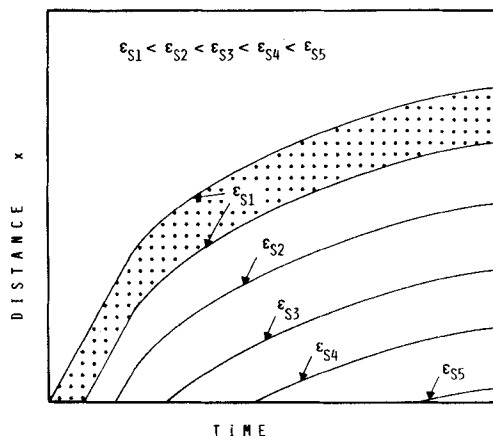


Figure 7. Lines of constant solids concentration in sediment.

the sediment at time t_1 , its value can be calculated by the following expression

$$V_s = \int_0^{L_1} \epsilon_s(z) dz \quad (20)$$

From Eq. 20

$$\frac{dV_s}{dt_1} = \int_0^{L_1} \frac{\partial \epsilon_s(z)}{\partial t_1} dt_1 + \epsilon_s(L_1) \frac{dL_1}{dt_1} \quad (21)$$

where $\epsilon_s(L_1)$ is the volume fraction of solids at the bottom of the column (which is at the distance L_1 from the sediment surface). In this hypothetical situation, however, $\partial \epsilon_s(z)/\partial t_1$ is zero because $\epsilon_s(z)$ depends only on the distance to the sediment surface z , and consequently $\epsilon_s(z)$ does not depend on time t_1 . Then,

$$\frac{dV_s}{dt_1} = \epsilon_s(L_1) \frac{dL_1}{dt_1} \quad (22)$$

V_s can also be worked out as

$$V_s = \int_0^{L_1} \epsilon_s(x) dx \quad (23)$$

and therefore

$$\frac{dV_s}{dt_1} = \epsilon_{s1} \frac{dL_1}{dt_1} + \int_0^{L_1} \frac{\partial \epsilon_s(x)}{\partial t_1} dx \quad (24)$$

Taking into account that the righthand side of Eq. 24 equals the lefthand member of Eq. 1, from Eqs. 1, 18, and 24 one deduces

$$\frac{dV_s}{dt_1} = \frac{dL_1}{dt_1} \phi_{s2} \left(1 + \frac{-u_{s2}}{\frac{dL_1}{dt_1}} \right) = \frac{dL_1}{dt_1} \epsilon_{su} \quad (25)$$

From Eqs. 22 and 25

$$\epsilon_s(L_1) = \epsilon_{su} \quad (26)$$

Therefore, in the assumed hypothetical situation the volume fraction of solids ϵ_s at the bottom in a batch test equals the corre-

sponding ϵ_{su} , which is the solids volume fraction of the designed thickener underflow, if the composition of the layer just above the thickener discontinuity is equal to the composition of the layer just above the compression discontinuity in the batch test.

In tests where the different layers of the sediment reach the maximum solids concentration quickly, in accordance with the squeeze transmitted by the upper layers, the method proposed previously enables us to estimate the situation of the lines of equal concentration in the sediment formed in a batch test.

Experimental Results

In order to test the model discussed above, calcium carbonate suspensions were chosen because it is possible to observe the level of the sediment directly, and because the initial tests carried out with these suspensions showed that the experimental data were almost exactly reproducible when the test was duplicated.

The chemical composition of the commercial calcium carbonate used is the following:

$\text{CaCO}_3 = 98.47 \text{ wt. } \%$

$\text{MgCO}_3 = 1.00 \text{ wt. } \%$

$\text{Fe}_2\text{O}_3 = 0.016 \text{ wt. } \%$

$\text{Al}_2\text{O}_3 = 0.20 \text{ wt. } \%$

$\text{SiO}_2 = 0.22 \text{ wt. } \%$

It was tested by microscopy that the greatest particle diameter was less than $20 \mu\text{m}$. The particle density was $2,580 \text{ kg/m}^3$, measured with water and benzene using a pycnometer.

The experiments were carried out in a 1 L graduated cylinder at 20°C . For measuring the heights of the discontinuities in a fixed vertical line, a magnifying glass was used. In some experiments KMnO_4 was added to the suspension in order to observe more clearly the level of the sediment. The KMnO_4 concentration was always less than $0.01 \text{ wt. } \%$. With these concentrations the experimental data obtained from the test performed with and without KMnO_4 show no influence of the ionic salt on the settling rates.

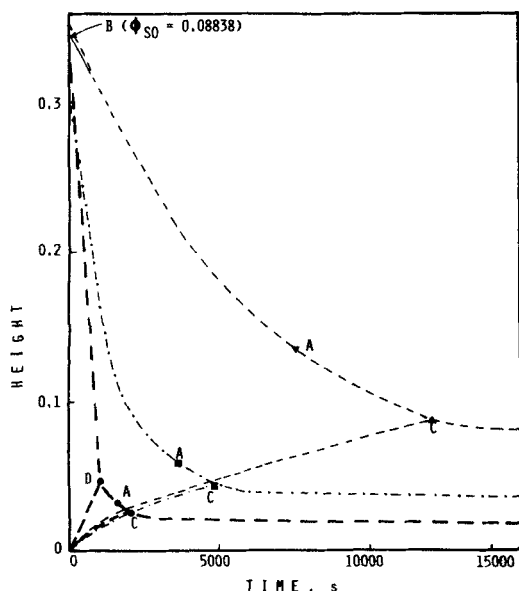


Figure 8. Discontinuity heights vs. time.

— $\phi_{so} = 0.0200$; --- $\phi_{so} = 0.04417$; - · - $\phi_{so} = 0.08838$

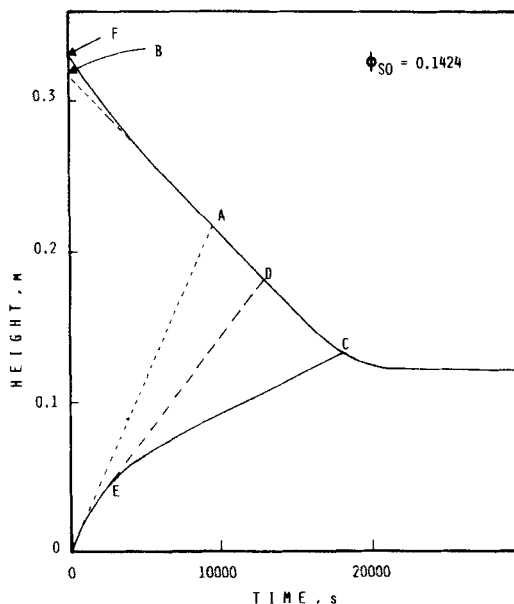


Figure 9. Discontinuity heights vs. time.

$\phi_{so} = 0.1424$

The discontinuity heights of the experiments carried out at different initial concentrations are plotted in Figures 8 and 9. In each curve point *A* is the intercept of the straight line drawn from the origin tangentially to the sediment curve, and the upper discontinuity. Point *B* is the intercept of the first constant settling rate line on the height axis. Point *C* is the critical point, where the cake surface meets the pulp-supernatant interface. In all cases there is a great change in the settling rate at point *C*.

In the curve corresponding to the smallest initial concentration of solids, a straight line of discontinuity (origin point *D*) between two concentrations in the settling zone has also been observed.

Points *B* are below the initial height H_o . In the tests of $\phi_{so} = 0.0200$ and $\phi_{so} = 0.04417$, points *B* are very close to the initial heights H_o . In order to obtain a uniform concentration initially, the suspension is agitated before beginning the test. It is known that the particles or their stable agglomerations are covered by a film of water when they fall through the suspension (Michaels and Bolger, 1962; Fitch, 1979). Agitation can cause a decrease in the thickness of the film of water, and this would explain why the initial settling rates are greater than the rates observed after a short period, as can be noted in Figures 8 and 9. This effect is more pronounced at high solids concentration because the film of water around the particles modifies to a greater extent the real volume fraction of free water (where free water circulates upward). In all calculations in this work the initial heights H_o are those corresponding to points *B*. We can observe in the experimental curve of $\phi_{so} = 0.0200$ that the small perturbations in the initial period do not affect the rise of the origin point *D* discontinuity, and probably also do not affect the rise of the characteristics from the origin or from the sediment.

Value ϵ_{s1}

Using Eq. 20, values of ϵ_{s1} , the volume fraction of solids at the cake surface, have been worked out from the experimental data

of the tests whose initial ϕ_{so} are 0.0200, 0.04417, and 0.08838. They are presented in Table 1.

Note that the sediment height curves of the tests plotted in Figure 8 almost coincide. This is to be expected as the characteristics that rise from the sediment are identical and their ascents do not depend on the initial height and on the initial concentration. In Table 1, values ϕ_{s2}^* corresponding to the characteristic that rises from the bottom tangentially to the sediment curve for each test are also shown.

In the test shown in Figure 9 ($\phi_{so} = 0.1424$) the velocity of the rising sediment at the beginning of the test is greater than those of Figure 8, for two reasons. First, the solids that form the sediment come from layers of $\phi_{so} = 0.1424$, which is greater than the values ϕ_{s2}^* presented in Table 1. Second, the initial settling rate, which is high due to the initial turbulence, causes an increase in the rise velocity of the cake surface. For the test of Figure 9, taking into account that the volume fractions of solids just above and below the compression discontinuity are ϕ_{so} and ϵ_{s1} , respectively, and that u_{s1} equals zero at $t_1 = 0$, Eq. 5 yields

$$\epsilon_{s1} = \frac{\phi_{so} \left[\left(-\frac{dH_2}{dt_2} \right)^o + \left(\frac{dL_1}{dt_1} \right)^o \right]}{\left(\frac{dL_1}{dt_1} \right)^o} \quad (27)$$

where $(-dH_2/dt_2)^o$ is the slope of the tangent to the curve $H_2 = f(t_2)$ at point F and $(dL_1/dt_1)^o$ is the slope of the line origin point A .

Note that the different values of ϵ_{s1} shown in Table 1 are similar.

Settling flux

In Figure 10 values of $(-u_s)\phi_s$ are plotted vs. ϕ_s . The values have been obtained by two different procedures:

1. From the tests presented in Figure 8 using Eq. 6 or 9
2. From the slope of the straight line in the height vs. time plot of some tests

The method of Coe and Clavenger (1916) for determining thickener unit area requires performing several tests with different initial volume fractions of solids. Using some suspensions, for example, commercial calcium carbonate suspensions, the correct settling rate u_{so} may be determined only after an initial period. Moreover the initial height H_o must be great enough to prevent characteristics of ϕ_{s2} greater than ϕ_{so} from reaching the upper discontinuity during the determination period for the settling rate u_{so} . In Figure 9 the line ED has a slope corresponding to the characteristic with volume fraction of solids equal to the initial one. To the right of this line, characteristics of ϕ_{s2} values greater than ϕ_{so} can be drawn. If H_o had been 0.2 m, an incorrect value of the corresponding settling rate would have been obtained.

Table 1. Parameter Values

ϕ_{so}	ϵ_{s1}	ϕ_{s2}^*	ϵ_{su}^{\max}	L_c/L_{∞}	$(\epsilon_{so})_{avg}$
0.02000	0.216	0.121	—	1.302	0.360
0.04417	0.220	0.125	0.364	1.273	0.391
0.08838	0.229	0.130	0.398	1.161	0.406
0.1424	0.227	—	—	1.134	0.406

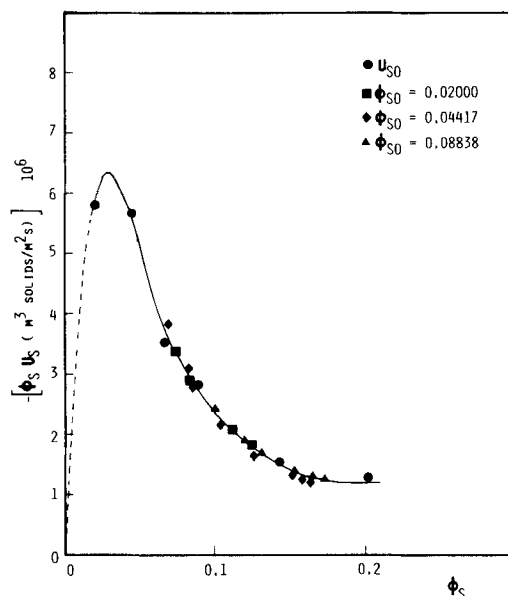


Figure 10. Settling flux vs. volume fraction of solids.

In view of Figure 10, we can observe that the different values, obtained by the two procedures cited before, are coincident. The shape of the curve plotted in Figure 10 also justifies the presence of the discontinuity corresponding to the line OD in Figure 8 for the test of $\phi_{so} = 0.0200$, in accordance with Kynch's theory.

Comparison of Equations to Calculate ϕ_{s2}

Three equations are considered to calculate the values ϕ_{s2} corresponding to the layers whose characteristics rise from the sediment. These are Eqs. 28, 29, and 30.

$$\phi_{s2} = \frac{\phi_{so} H_o}{H_{12} - L_1} \exp \left(- \int_0^{t_1} \frac{1}{t_2 - t_1} dt_1 \right) \quad (28)$$

Equation 28 is the one deduced in this paper.

$$\phi_{s2} = \frac{\phi_{so} H_o}{H_i} \quad (29)$$

The values ϕ_{s2} obtained from Eq. 29 would be the corresponding ones if all the characteristics rose from the bottom of the column, and $L_1 = f(t_1)$ would be a straight line between the origin and the critical point.

$$\phi_{s2} = \phi_{so} \frac{H_o - H_j}{H_i - H_j} \quad (30)$$

Equation 30 is that proposed by Fitch (1983). This equation has been deduced by drawing the characteristic tangent to the sediment surface curve from the height axis.

From the tests of $\phi_{so} = 0.04417$ and $\phi_{so} = 0.08838$, some values of u_{s2} ($= dH_2/dt_2$) and the corresponding values of ϕ_{s2} calculated by Eqs. 28, 29, and 30 are shown in Table 2. In Appendix III of the supplementary material the calculus procedure is commented on. In Table 2 the values of ϕ_{s2} are presented to four decimal figures in order to compare the results obtained by the different methods.

Table 2. Values of $-dH_2/dt_2$ and ϕ_{s2}

$-dH_2/dt_2$ m/s	ϕ_{s2} Calc. by		
	Eq. 28	Eq. 29	Eq. 30
Exp., $\phi_{s0} = 0.04417$			
9.014×10^{-6}	0.1502	0.1492	0.1566
8.166×10^{-6}	0.1577	0.1563	0.1664
7.941×10^{-6}	0.1599	0.1582	0.1691
7.720×10^{-6}	0.1624	0.1605	0.1826
Exp., $\phi_{s0} = 0.08838$			
1.233×10^{-5}	0.1347	0.1347	0.1349
9.564×10^{-6}	0.1512	0.1511	0.1537
9.250×10^{-6}	0.1541	0.1539	0.1576
8.222×10^{-6}	0.1643	0.1634	0.1705
7.487×10^{-6}	0.1732	0.1713	0.1814

In view of Table 2, note that the values of ϕ_{s2} calculated by Eq. 28 are between those obtained using Eqs. 29 and 30. This is not accidental; mathematically it can be demonstrated as shown in Appendix II of the supplementary material.

Unit Area of Continuous Thickener

The unit area for calcium carbonate suspension thickener is worked out by various procedures using the experimental data of the tests performed with $\phi_{s0} = 0.04417$ and $\phi_{s0} = 0.08838$:

1. From the equations presented in this paper, based on Eq. 28 or 9
2. By the Talmadge and Fitch (1955) method based on Eq. 29
3. By Fitch's (1983) method based on Eq. 30

The calculus procedure is presented in Appendix III, supplementary material.

In Figures 11 and 12 the unit areas A_u are plotted vs. the underflow concentration ϵ_{su} . Note that:

- By Fitch's method, the values of A_u are smaller than those worked out by the method presented in this paper
 - The values of A_u obtained using Talmadge and Fitch's method are slightly greater than the ones calculated by the method considered in this work, but the value ϵ_{su}^{max} (corresponding to the critical point) is less than that calculated by the procedure proposed in this paper
 - By extrapolation of the Talmadge and Fitch method, when it is necessary to draw the tangent by the critical point, the values of A_u are also slightly greater than those obtained by the method presented here (points \square in Figures 11 and 12)
- In the latter case it is not possible to ascertain a limit for the value ϵ_{su}^{max} from the batch test. Identical results would be obtained from the Yoshioka construction, taking into account the values of ϕ_{s2} worked out using Eqs. 28, 29, and 30.

Consequently, by the Talmadge and Fitch method, the values of A_u worked out are greater than necessary. By this method, however, it is not possible to calculate the upper limit of ϵ_{su} , when the extrapolation of the method is considered. This would justify the satisfactory results obtained by the Talmadge and Fitch method in many cases, and the failures in others.

The values of ϵ_{su}^{max} , L_c/L_∞ , and the mean volume fractions of solids $\epsilon_{s\infty}$ (at time = 3 days) are also shown in Table 1. It may be observed in Figures 11 and 12 that the intervals of ϵ_{su} are wide enough to consider the optimal design of the continuous thickener. For the same values of ϵ_{su} , the differences between the values

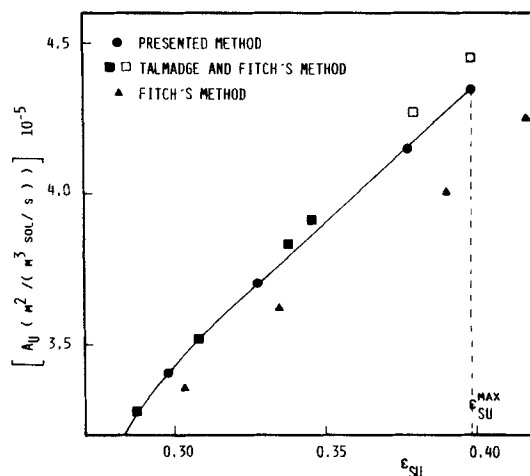


Figure 11. Unit area of continuous thickener vs. underflow concentration.
 $\phi_{s0} = 0.04417$

of A_u calculated from the experimental data of $\phi_{s0} = 0.04417$ and $\phi_{s0} = 0.08838$ are less than 10%, using the method proposed in this paper.

With the calcium carbonate suspensions used, the differences between the values of A_u calculated by the three methods are not very large. However with other suspensions, whose settling hydrodynamics in the sediment are distinct, the differences could be greater.

Estimation of Sediment Height vs. Time Curve

When it is not possible to measure the sediment height, an estimation of the sediment height at each time can be obtained from only two tests. The initial heights or the initial concentrations must be different in order to obtain two distinct curves of the upper discontinuity. The procedure is applied in Figure 13 to the experimental data of the tests performed with the solids concentrations $\phi_{s0} = 0.04417$ and $\phi_{s0} = 0.08838$. In this figure, some

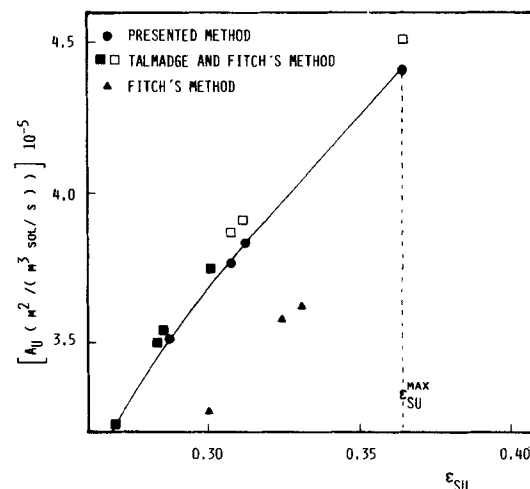


Figure 12. Unit area of continuous thickener vs. underflow concentration.
 $\phi_{s0} = 0.08838$

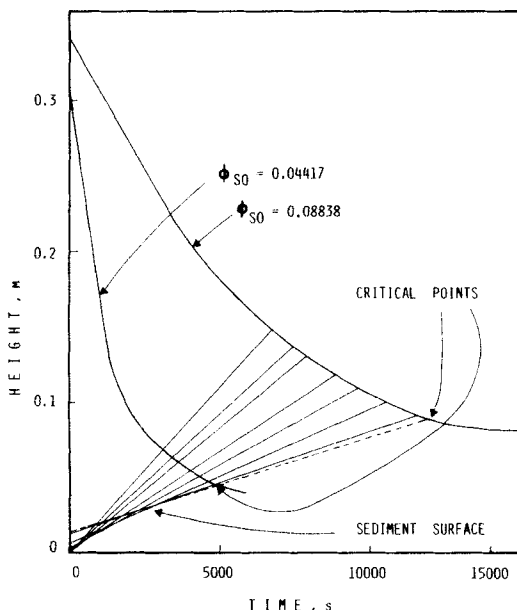


Figure 13. Estimated height of sediment surface vs. time.

straight lines joining points with the same settling rate of the upper discontinuities are drawn. Note that there are some lines that pass close to the origin, and others that intersect the height axis on the positive part. This means that some characteristics rise from the bottom of the cylinder, and others do so from the sediment. We can approximately draw the curve $L_1 = f(t_1)$ tangent to all the characteristics with positive ordinate at $t = 0$. Comparing the sediment surface curves of Figure 8 and 13, we deduce that they are almost coincident. This method assumes a knowledge of the situation of the critical points (which can be obtained from a great change in the settling rate). With the estimated curve $L_1 = f(t_1)$, the relations presented in this paper can be used.

Analysis of the Rise of the Characteristics

In this paper, it has been assumed that the characteristics rise tangentially from the sediment. The experimental results shown in Figure 8 and the procedure illustrated in Figure 13 seem to confirm this assumption, stated by Fitch (1983). If the rise of the characteristic depended on the initial concentration, then the respective sediment height curves of $\phi_{so} = .0200$, 0.04417 , and 0.08838 would be distinct. On the other hand, as the estimated sediment height curve in Figure 13 is very close to the experimental curves, the only possible explanation is that the characteristics rise tangentially to the sediment. The coincidence of the values $\delta_{s_2}^*$ and ϵ_{s1} , shown in Table I, also confirms this assumption.

Notation

A_u = unit area of continuous thickener, $m^2/(m^3 \text{ solids} \cdot s)$
 c_s = volume fraction of solids; ϕ_s in settling zone, ϵ_s in sediment
 H = height of descending interface, m
 H_i = intercept height of tangent to curve $H_2 = f(t_2)$ on x axis
 H_j = intercept height of tangent to curve $L_1 = f(t_1)$ on height axis, m/s

H_0 = initial value of H at $t = 0$, m
 H_1, H_2 = values of H at t_1 and t_2 , m
 H_{12} = intercept height between parallel line to x axis that passes through (t_1, L_1) and tangent to curve $H_2 = f(t_2)$, m
 L = sediment height
 L_1 = sediment height at t_1 , m
 L_c = sediment height at critical point, m
 L_∞ = sediment height at time infinite, m
 S = volumetric settling flux of solids = $u_s c_s$, $m^3/m^2 \cdot s$
 t = time, s
 t_1, t_2 = values of t at intersection of characteristic with sediment (t_1) and upper interface (t_2)
 u_s = settling velocity of solids, m/s
 u_{s0} = initial settling velocity of solids, m/s
 u_{s1} = sedimentation velocity of solids at top of sediment, m/s
 u_{s2} = value of u_s at upper interface; $u_{s2} = dH_2/dt_2$, m/s
 v = upward propagation rate of discontinuity, m/s
 v_c = upward propagation rate of compression discontinuity, m/s
 v_u = downward velocity of pulp in continuous thickening resulting from underflow withdrawal, m/s
 V_s = volume of solids in sediment by unit of cross section, m^3/m^2
 x = distance down column; $dx = -dH$, m
 z = distance to sediment surface, m

Greek letters

ϵ_s = volume fraction of solids in sediment
 ϵ_{s1} = value of ϵ_s at cake surface
 ϵ_{su} = underflow volume fraction of solids
 ϵ_{su}^{max} = maximum value of ϵ_{su}
 $\epsilon_{s\infty}$ = volume fraction of solids in sediment at time infinite
 ν_1 = characteristic velocity at t_1 , m/s
 ϕ_s = volume fraction of solids in suspension
 ϕ_{s0} = initial suspension concentration
 ϕ_{s2} = value of ϕ_s corresponding to layers that arise from sediment
 ϕ_{s2}^* = of characteristic that rises from bottom tangentially to sediment

Symbols

$()_{avg}$ = mean value or average
 $()^o$ = corresponding to values of Figure 9
 $()^*$ = value related to characteristic that rises from bottom of column tangentially to sediment

Literature Cited

- Coe, H. S., and G. H. Clevenger, "Methods for Determining the Capacities of Slime-Settling Tanks," *Trans., Am. Inst. Min. Eng.*, **60**, 356 (1916).
d'Avila, J. S., and R. Sampaio, "Algumas consideracoes sobre o problema da sedimentacao," *VII Encontro sobre Escoamento em Meios Porosos*, Rio Clara, SP, COPPE, Caixa Postal 1191, ZC-00,20000 Rio de Janeiro, RJ, Brazil (1979).
Fitch, B., "Current Theory and Thickener Design," *Ind. Eng. Chem.*, **58**, 18 (1966).
———, "Current Theory and Thickener Design. 1, 2, 3," *Filtration and Separation*, **12**, 355, 480, 636 (1975).
———, "Sedimentation of Flocculent Suspensions: State of the Art," *AIChE J.*, **25**, 913 (1979).
———, "Letter to the Editor," *AIChE J.*, **28**(5), 871 (1982).
———, "Kynch Theory and Compression Zones," *AIChE J.*, **29**, 940 (1983).
Kynch, G. J., "A Theory of Sedimentation," *Trans. Faraday Soc.*, **48**, 166 (1952).
Michaels, A. S., and J. C. Bolger, "Settling Rates and Sediment Volumes of Flocculated Kaolin Suspensions," *Ind. Eng. Chem. Fundam.*, **1**, 24 (1962).
Scott, K. J., "Mathematical Models of Mechanism of Thickening," *Ind. Eng. Chem. Fundam.*, **5**, 109 (1966).
———, "Thickening of Calcium Carbonate Slurries," *Ind. Eng. Chem. Fundam.*, **7**, 484 (1968).

Talmadge, W. P., and E. B. Fitch, "Determining Thickener Unit Area," *Ind. Eng. Chem.*, **47**, 38 (1955).

Tiller, F. M., "Revision of Kynch Sedimentation Theory," *AIChE J.*, **27**, 823 (1981).

Yoshioka, N., Y. Hotta, S. Tanaka, S. Naito, and S. Tsugami, "Continuous Thickening of Homogeneous Flocculated Slurries," *Kagaku Kogaku*, **21**, 66 (1957).

Manuscript received Feb. 24, 1986, and revision received Aug. 12, 1987.

See NAPS document no. 04549 for 8 pages of supplementary material. Order from NAPS c/o Microfiche Publications, P.O. Box 3513, Grand Central Station, New York, NY 10163. Remit in advance in U.S. funds only \$7.75 for photocopies or \$4.00 for microfiche. Outside the U.S. and Canada, add postage of \$4.50 for the first 20 pages and \$1.00 for each of 10 pages of material thereafter, \$1.50 for microfiche postage.